

Supersymmetric Scaling Violations and UHECR.^a
(The Distribution and Fragmentation functions
of $N = 1$ QCD)

Claudio Corianò

Theory Group, Phys. Dept.

Univ. of Lecce

and

Istituto Nazionale di Fisica Nucleare

Sezione di Lecce

Via Arnesano, 73100 Lecce, Italy

^abased on joint work with Alon Faraggi(Oxford, UK)

ABSTRACT:

Moving QCD toward the astroparticle boundary generates new challenges for perturbation theory, such as the presence of Large Evolution Scales.

Fragmentation Regions/Initial state Scaling Violations at such energies may require -if we believe in supersymmetry- a better understanding of the supersymmetric DGLAP and the Supersymmetric Parton Model.

Heavy Relics Decays in Susy QCD (C.C., Alon Faraggi (Oxford)), to appear

**Supersymmetric Scaling Violations (1).
An Algorithm to solve the Supersymmetric
DGLAP Evolution**

(C.C. Sep 2000. hep-ph/0009227)

**Supersymmetric Scaling Violations (2).
The General Supersymmetric Evolution**
(C.C. Oxford Feb 2001. hep-ph/0102164)

**Supersymmetric Scaling Violations (3).
Supersymmetric Sum Rules**
(C.C., to appear)

Objective:

We try to underline a phenomenological program in astroparticle physics where standard QCD tools (evol. eqs.) may play a relevant role. Same tools can be applied for studies of QCD @ LHC (supersymmetric Jets, Susy Color Ordering etc..)

Context:

Ultra

High

Energy

Cosmic

Rays

Experimental Motivations:

- Cosmic Ray Particles with energies in excess of 4×10^{11} GeV have been detected

HAVERAH PARK

FLY's EYE

AKENO GIANT AIR SHOWER ARRAY (AGASA)

Hystorical Note

1966

In the early 1960s, Arno Penzias and Robert Wilson discovered that low-energy microwaves permeate the universe. Kenneth Greisen, Vadem Kuzmin and Georgi Zatsepin pointed out that high-energy cosmic rays would interact with the microwave background. The interaction would reduce their energy, so that particles traveling long intergalactic distances could not have energies greater than 5×10^{19} eV.

Mean free Path (MFP) of protons on the Cosmic Microwave Background (CMB)

decreases rapidly @ 3×10^{20} eV.

Even smaller (MFP) for nuclei.

GZK cutoff

1962

John Linsley and collaborators discovered the first cosmic ray with an energy of about 10^{20} eV in the Volcano Ranch array in New Mexico.

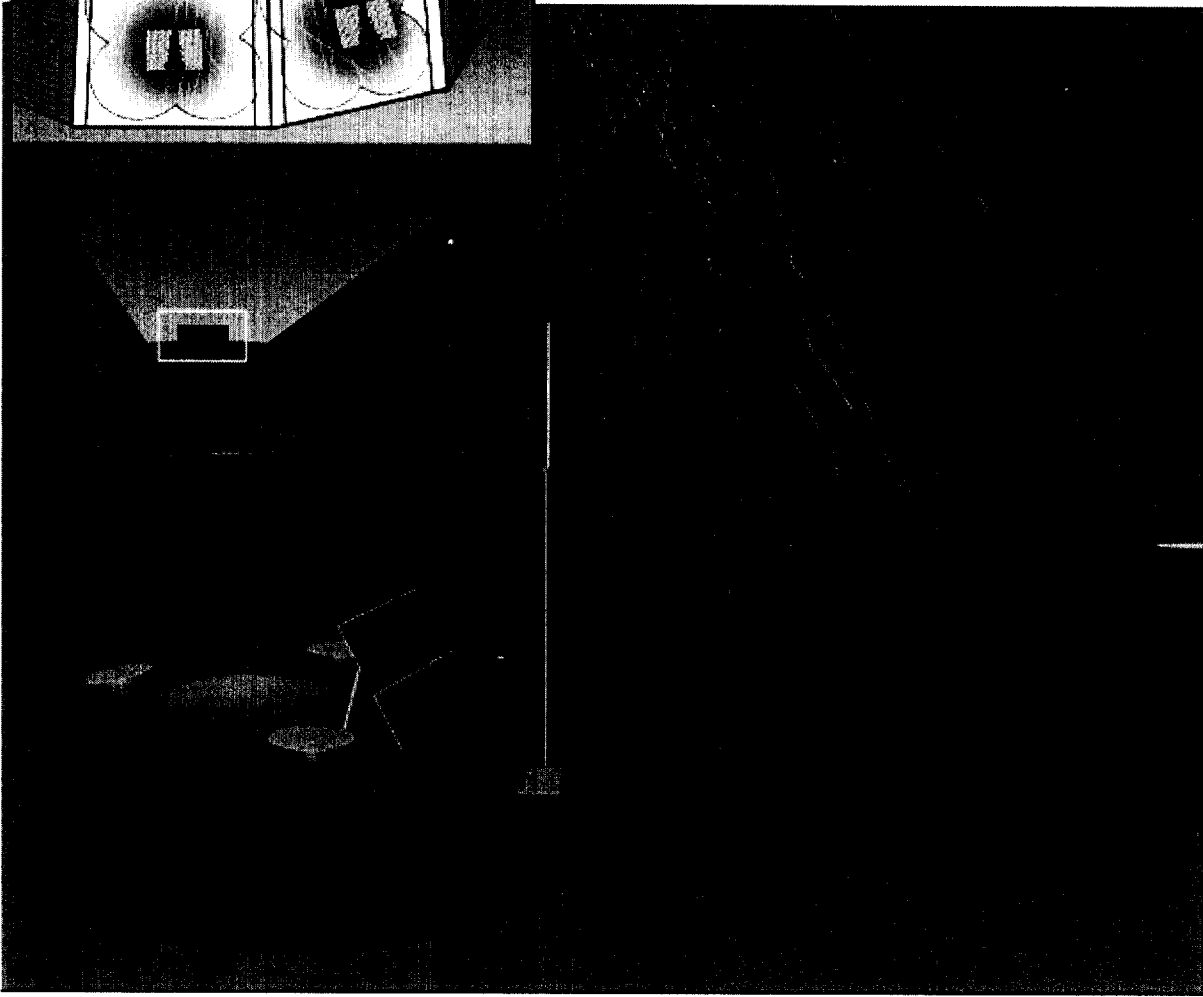
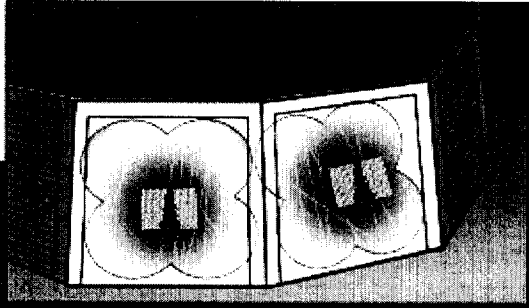
1991

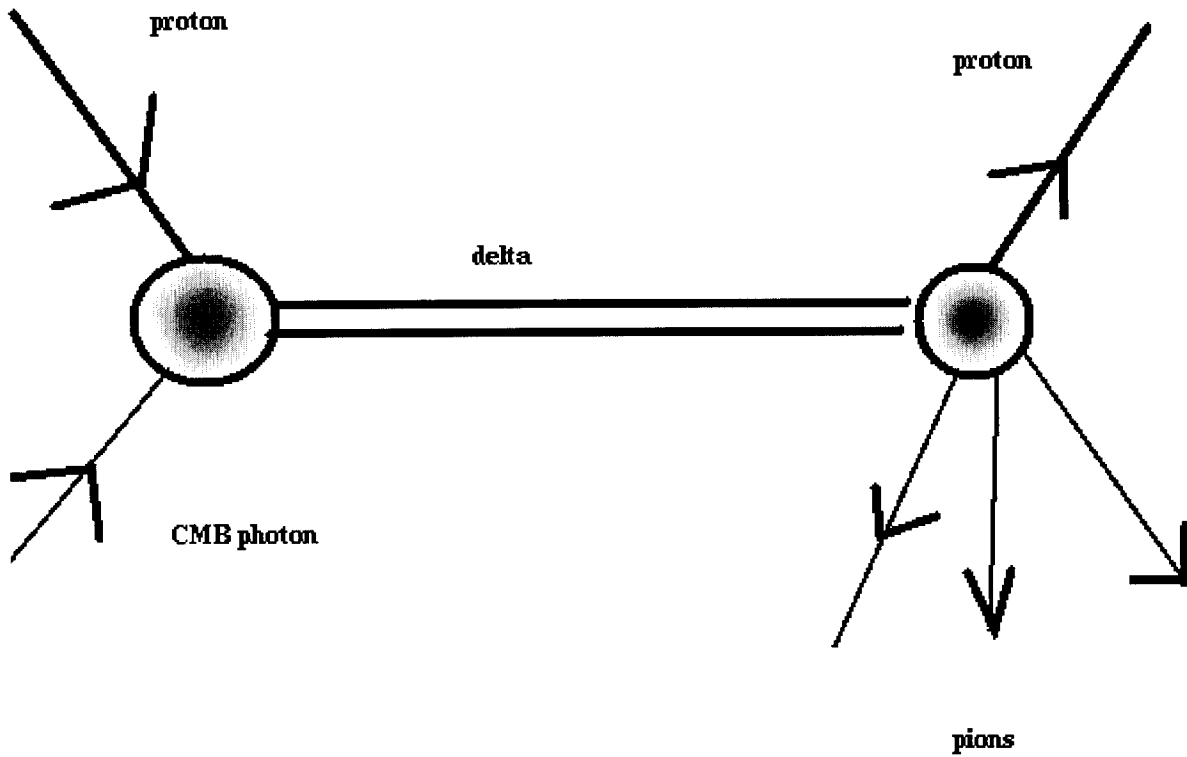
The Fly's Eye cosmic ray research group in the USA observed a cosmic ray event with an energy of 3×10^{20} eV. Events with energies of 10^{20} eV had been reported in the previous 30 years, but this was clearly the most energetic.

1994

The AGASA Group in Japan and the Yakutsk group in Russia each reported an event with an energy of 2×10^{20} eV. The Fly's Eye event and these events are higher in energy than any seen before. *Who ordered them?*

The Pierre Auger Project will construct two 3000 square kilometer grids of detectors spaced at 1.5 kilometer intervals. One array in the Northern Hemisphere and a second in the Southern Hemisphere.





Production of single and multiple pions
until $E_p < E_{GZK}$
after which protons propagate freely.

From detailed simulations: Primaries are protons.

Integrated Flux well described by a “local” power law

$$N(E) = \frac{K}{E^x} \quad (1)$$

The description is fine in a very large range $1 \text{ GeV} < E < 5 \times 10^{11} \text{ GeV}$. Total flux changes dramatically

$$\Phi(E = 100 \text{ GeV}) \approx 1 \text{ particle/km}^2 \text{ sec} \quad (2)$$

$$\Phi(E = 10^{11} \text{ GeV}) \approx 1 \text{ particle/km}^2 \text{ century} \quad (3)$$

up to 1 TeV good discrimination of the various components through direct detection.

protons \rightarrow .87

helium \rightarrow .12

heavier \rightarrow nuclei .01

- Differences between species understood in terms of source production and propagation.
- Relative abundances modified by the interstellar medium (i.e. spallation)

Spectral index:

- $x \approx 2.5$ ($10^3 - 10^4$ GeV) (flattens)
- steepens fairly dramatically above this range
(diffusion of cosmic rays from galaxy, difficult to contain at these energies)
- $x \approx 3.08$ ($10^7 - 10^{11}$ GeV)
- The composition is difficult to detect directly
(dominated by protons) (flattening/steeping
→ knee)
- $E < 10^{11}$ $x \approx 3.16$ (steeping)
- $E > 10^{11}$ $x \approx 2.78$ (flattening)
- (steeping/flattening → ankle)

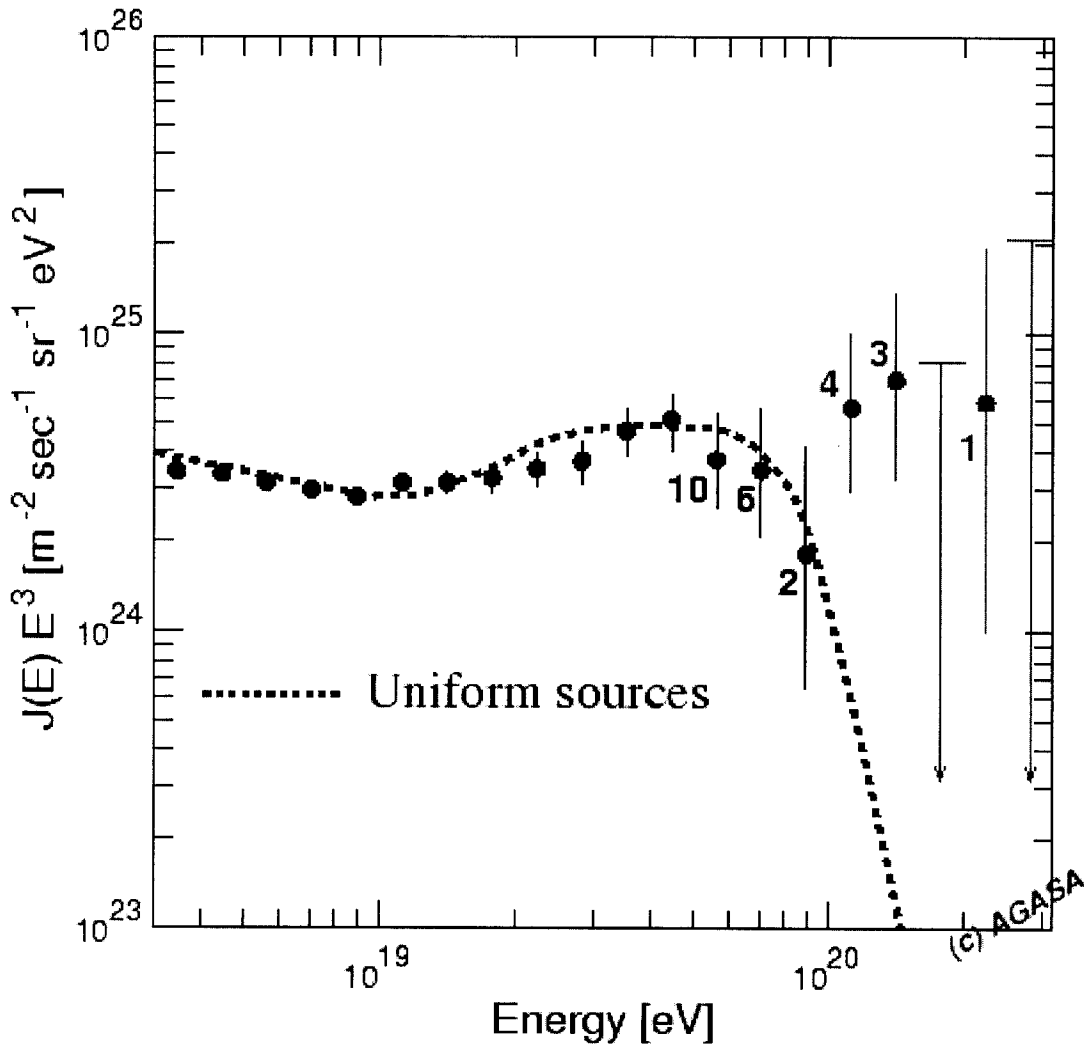
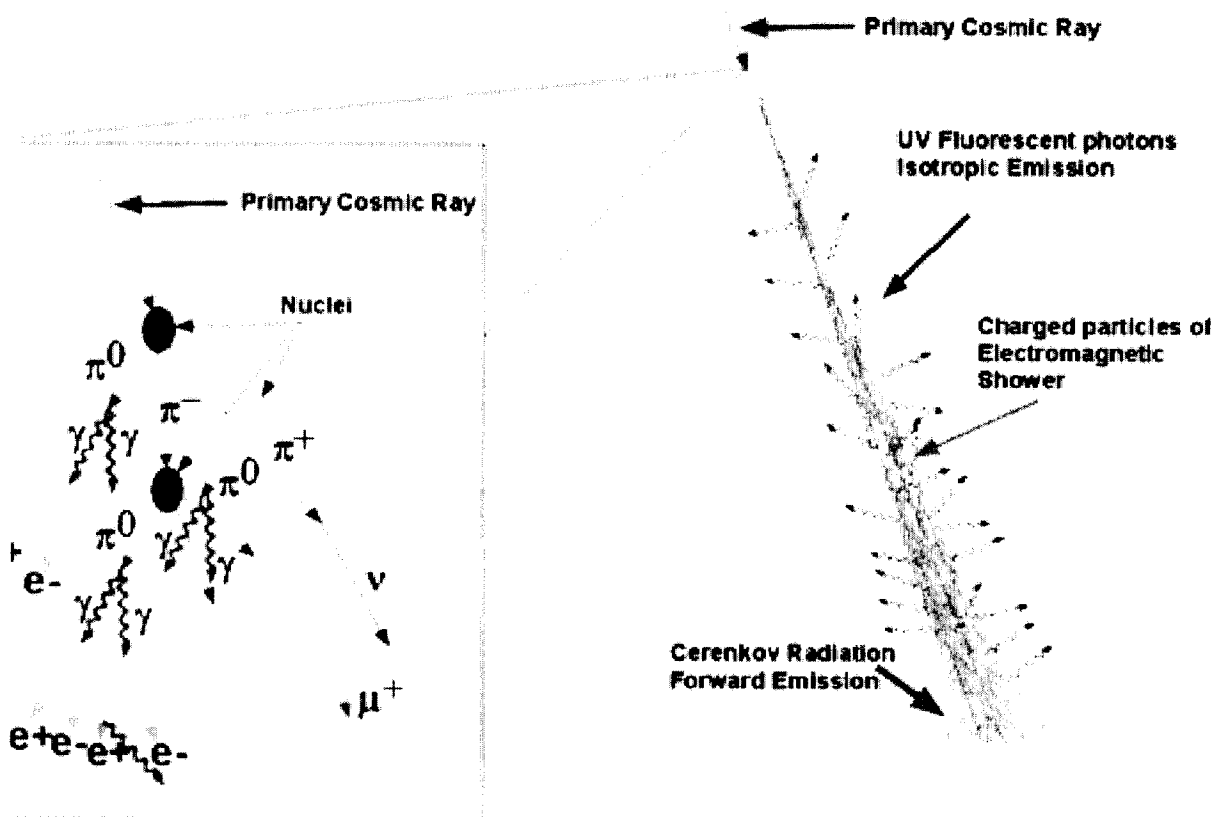
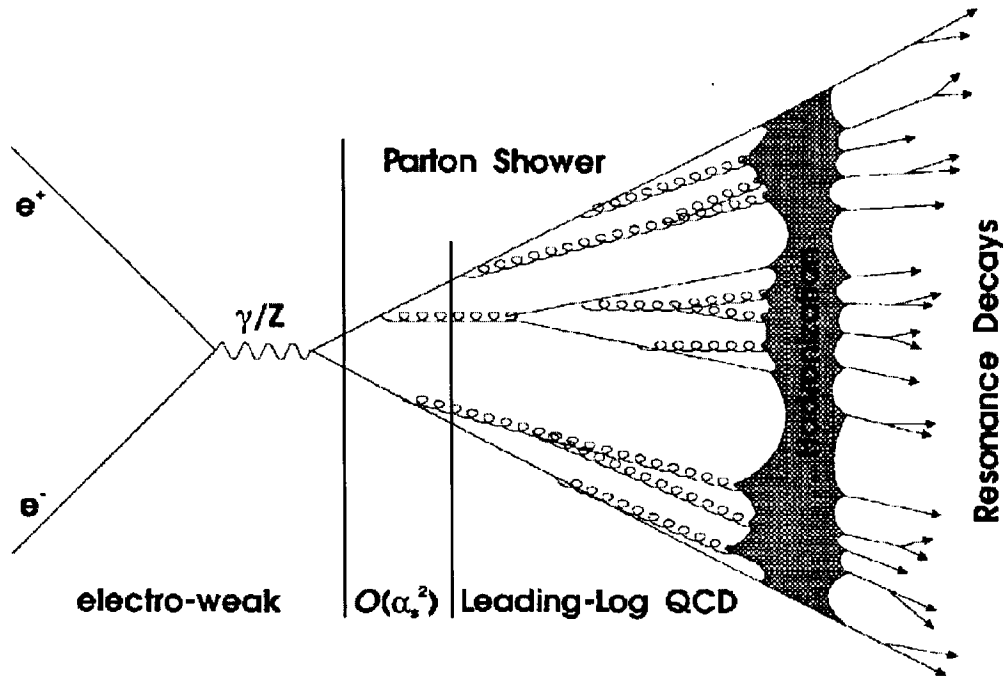


Figure 1: AGASA Spectrum





Two Scales for QCD

A High Energy Λ_F fragmentation Scale
 $\approx 10^{11}$ (decay of a metastable state \rightarrow
 primaries protons)

A collision scale Λ_{coll} due to the interaction
 of surviving primaries with air-nuclei
 ($E \approx 400 TeV$)

At both scales supersymmetric scaling violations
 should be included and the multiplicities of the
 spectrum analyzed. The DGLAP evolution covers
 all the regions, starting from the originally
 metastable state

I) fragmenting region \rightarrow primaries (evolution of
 the fragmentation functions) II) collision region
 (initial state scaling violations (susy pdf's))

QCD DGLAP

The evolution equations are of the form

$$\begin{aligned}
 Q^2 \frac{d}{dQ^2} q_i^{(-)}(x, Q^2) &= \frac{\alpha(Q^2)}{2\pi} P_{(-)}(x, \alpha(Q^2)) \otimes q_i^{(-)}(x, Q^2) \\
 Q^2 \frac{d}{dQ^2} \chi_i(x, Q^2) &= \frac{\alpha(Q^2)}{2\pi} P_{(-)}(x, \alpha(Q^2)) \otimes \chi_i(x, Q^2),
 \end{aligned}
 \tag{1}$$

with

$$\chi_i(x, Q^2) = q_i^{(+)}(x, Q^2) - \frac{1}{n_F} q^{(+)}(x, Q^2) \tag{2}$$

for the non-singlet distributions and

$$Q^2 \frac{d}{dQ^2} \begin{pmatrix} q^{(+)}(x, Q^2) \\ G(x, Q^2) \end{pmatrix} = \begin{pmatrix} P_{qq}(x, Q^2) & P_{qg}(x, Q^2) \\ P_{gq}(x, Q^2) & P_{gg}(x, Q^2) \end{pmatrix} \otimes \begin{pmatrix} q^{(+)}(x, Q^2) \\ G(x, Q^2) \end{pmatrix} \tag{3}$$

for the singlet sector.

We have defined, as usual

$$q_i^{(-)} = q_i - \bar{q}_i, \quad q_i^{(+)} = q_i + \bar{q}_i, \quad q^{(+)} \equiv \Sigma = \sum_{i=1}^{n_f} q_i^{(+)}. \tag{4}$$

We introduce the evolution variable

$$t = -\frac{2}{\beta_0} \ln \frac{\alpha(Q^2)}{\alpha(Q_0^2)} \tag{5}$$

which replaces Q^2 . The evolution equations are then rewritten in the form

$$\begin{aligned}
\frac{d}{dt} q_i^{(-)}(t, x) &= \left(P^{(0)}(x) + \frac{\alpha(t)}{2\pi} R_{(-)}(x) + \dots \right) \otimes q_i^{(-)}(t, x) \\
Q^2 \frac{d}{dt} \chi_i(x, Q^2) &= \left(P^{(0)}(x) + \frac{\alpha(t)}{2\pi} R_{(-)}(x) \right) \otimes \chi_i(x, Q^2), \\
\frac{d}{dt} \begin{pmatrix} q^{(+)}(t, x) \\ G(x, t) \end{pmatrix} &= \left(P^{(0)}(x) + \frac{\alpha(t)}{2\pi} R(x) + \dots \right) \otimes \begin{pmatrix} q^{(+)}(x, t) \\ G(x, t) \end{pmatrix}.
\end{aligned} \tag{6}$$

QCD Fragmentation

The equations for the fragmentation functions in QCD are given by

$$\begin{aligned}
\frac{d}{d \log(Q^2)} D_{q_i}^h(x, Q^2) &= \frac{\alpha(Q^2)}{2\pi} \left(P_{qq} \otimes D_{q_i}^h + \frac{1}{2n_f} P_{gq} \otimes D_g^h \right) \\
\frac{d}{d \log(Q^2)} D_g^h(x, Q^2) &= \frac{\alpha(Q^2)}{2\pi} \left(P_{qg} \otimes \sum_i (D_{q_i}^h + D_{\bar{q}_i}^h) + P_{gg} \otimes D_g^h \right)
\end{aligned} \tag{7}$$

The evolution of the fragmentation functions is also decomposed into a non singlet and in a singlet sector

$$Q^2 \frac{d}{dQ^2} D_{q_i^{(-)}}^h(x, Q^2) = \frac{\alpha(Q^2)}{2\pi} P_{qq}(x, \alpha(Q^2)) \otimes D_{q_i^{(-)}}^h(x, Q^2) \tag{8}$$

for the non-singlet distributions and

$$\frac{d}{d \log(Q^2)} \begin{pmatrix} D_{q^{(+)}}^h(x, Q^2) \\ D_g^h(x, Q^2) \end{pmatrix} = \begin{pmatrix} P_{qq} & P_{gq} \\ P_{qg} & P_{gg} \end{pmatrix} \otimes \begin{pmatrix} D_{q^{(+)}}^h(x, Q^2) \\ D_g^h(x, Q^2) \end{pmatrix} \tag{9}$$

for the singlet sector, where

$$D_{q_i^{(-)}}^h(x, Q^2) = D_{q_i}^h - D_{\bar{q}_i}^h \quad (10)$$

1 The Supersymmetric DGLAP Evolution

The evolution equations can be separated in two non-singlet sectors and a singlet one. The non-singlet are

$$\begin{aligned}
 Q^2 \frac{d}{dQ^2} q_V(x, Q^2) &= \frac{\alpha(Q^2)}{2\pi} (P_{qq} \otimes q_V + P_{q\tilde{q}} \otimes \tilde{q}_V) \\
 Q^2 \frac{d}{dQ^2} \tilde{q}_V(x, Q^2) &= \frac{\alpha(Q^2)}{2\pi} (P_{\tilde{q}q} \otimes q_V + P_{\tilde{q}\tilde{q}} \otimes \tilde{q}_V),
 \end{aligned}
 \tag{11}$$

and the singlet, which mix q_V and \tilde{q}_V with the gluons and the gluinos are

$$Q^2 \frac{d}{dQ^2} \begin{bmatrix} G(x, Q^2) \\ \lambda(x, Q^2) \\ q^+(x, Q^2) \\ \tilde{q}^+(x, Q^2) \end{bmatrix} = \begin{bmatrix} P_{GG} & P_{G\lambda} & P_{Gq} & P_{G\tilde{q}} \\ P_{\lambda G} & P_{\lambda\lambda} & P_{\lambda q} & P_{\lambda\tilde{q}} \\ P_{qG} & P_{q\lambda} & P_{qq} & P_{qs} \\ P_{sG} & P_{s\lambda} & P_{\tilde{q}q} & P_{\tilde{q}\tilde{q}} \end{bmatrix} \otimes \begin{bmatrix} G(x, Q^2) \\ \lambda(x, Q^2) \\ q^+(x, Q^2) \\ \tilde{q}^+(x, Q^2) \end{bmatrix}.
 \tag{12}$$

2 Timelike Evolution

The equations for the timelike evolution are given by

$$\begin{aligned}
\frac{d}{d \log(Q^2)} D_g^h(x, Q^2) &= P_{gg} \otimes D_g^h + P_{\lambda g} \otimes D_\lambda^h + P_{qg} \otimes \sum_i (D_{q_i}^h + D_{\bar{q}_i}^h) \\
&\quad + P_{\bar{q}g} \otimes \sum_i (\tilde{q}_{iL} + \tilde{q}_{iR} + \bar{\tilde{q}}_{iL} + \bar{\tilde{q}}_{iR}) \\
\frac{d}{d \log(Q^2)} D_\lambda^h(x, Q^2) &= P_{g\lambda} \otimes D_g^h + P_{\lambda\lambda} \otimes D_\lambda^h + P_{q\lambda} \otimes \sum_i (D_{q_i}^h + D_{\bar{q}_i}^h) \\
&\quad + P_{s\lambda} \otimes \sum_i (\tilde{q}_{iL} + \tilde{q}_{iR} + \bar{\tilde{q}}_{iL} + \bar{\tilde{q}}_{iR}) \\
\frac{d}{d \log(Q^2)} D_{q_i}^h(x, Q^2) &= \frac{1}{2n_f} P_{gq} \otimes D_g^h + \frac{1}{2n_f} P_{\lambda q} \otimes D_\lambda^h + P_{\bar{q}q} \otimes (D_{\bar{q}_{iL}}^h + D_{\bar{q}_{iR}}^h) \\
&\quad + P_{qq} \otimes D_{q_i}^h \\
\frac{d}{d \log(Q^2)} D_{\bar{q}_{iL}}^h(x, Q^2) &= \frac{1}{4n_f} P_{g\bar{q}} \otimes D_g^h + \frac{1}{4n_f} P_{\lambda\bar{q}} \otimes D_\lambda^h + \frac{1}{2} P_{q\bar{q}} \otimes D_{q_i}^h \\
&\quad + P_{\bar{q}\bar{q}} \otimes D_{\bar{q}_{iL}}^h \\
\frac{d}{d \log(Q^2)} D_{\bar{q}_{iR}}^h(x, Q^2) &= \frac{1}{4n_f} P_{g\bar{q}} \otimes D_g^h + \frac{1}{4n_f} P_{\lambda s} \otimes D_\lambda^h + \frac{1}{2} P_{q\bar{q}} \otimes D_{q_i}^h \\
&\quad + P_{\bar{q}\bar{q}} \otimes D_{\bar{q}_{iR}}^h
\end{aligned} \tag{13}$$

Notation

$$D_{\bar{q}_i}^h(x, Q^2) \equiv D_{\bar{q}_{iL}}^h + D_{\bar{q}_{iR}}^h \tag{14}$$

to denote the fragmentation functions of squarks of flavour i at a fractional energy x and momentum Q .

It is also convenient to separate the equations, as usual, into singlet and non singlet sectors

$$\begin{aligned}
D_{q_V}^h(x, Q^2) &= \sum_{i=1}^{n_f} (D_{q_i}^h(x, Q^2) - D_{\tilde{q}_i}^h(x, Q^2)), \\
&\equiv D_{q_{NS}}^h \\
D_{\tilde{q}_V}^h(x, Q^2) &= \sum_{i=1}^{n_f} (D_{\tilde{q}_i}^h(x, Q^2) - D_{q_i}^h(x, Q^2)) \\
&\equiv D_{\tilde{q}_{NS}}^h \\
D_{q^+}(x, Q^2) &= \sum_{i=1}^{n_f} (D_{q_i}(x, Q^2) + D_{\tilde{q}_i}(x, Q^2)) \\
D_{\tilde{q}^+}(x, Q^2) &= \sum_{i=1}^{n_f} (D_{\tilde{q}_i}^h(x, Q^2) + D_{q_i}^h(x, Q^2)).
\end{aligned} \tag{15}$$

The non singlet equations are

$$\begin{aligned}
Q^2 \frac{d}{dQ^2} D_{q_V}(x, Q^2) &= \frac{\alpha(Q^2)}{2\pi} (P_{qq} \otimes D_{q_V}^h + P_{\tilde{q}\tilde{q}} \otimes D_{\tilde{q}_V}^h) \\
Q^2 \frac{d}{dQ^2} D_{\tilde{q}_V}(x, Q^2) &= \frac{\alpha(Q^2)}{2\pi} (P_{q\tilde{q}} \otimes D_{q_V}^h + P_{\tilde{q}\tilde{q}} \otimes D_{\tilde{q}_V}^h),
\end{aligned} \tag{16}$$

and the singlet matrix equations, which mix q_V and \tilde{q}_V with the gluons and the gluinos

$$Q^2 \frac{d}{dQ^2} \begin{bmatrix} D_G^h(x, Q^2) \\ D_\lambda^h(x, Q^2) \\ D_{q^+}^h(x, Q^2) \\ D_{\tilde{q}^+}^h(x, Q^2) \end{bmatrix} = \begin{bmatrix} P_{GG} & P_{G\lambda} & P_{Gq} & P_{G\tilde{q}} \\ P_{\lambda G} & P_{\lambda\lambda} & P_{\lambda q} & P_{\lambda\tilde{q}} \\ P_{qG} & P_{q\lambda} & P_{qq} & P_{qs} \\ P_{\tilde{q}G} & P_{\tilde{q}\lambda} & P_{\tilde{q}q} & P_{\tilde{q}\tilde{q}} \end{bmatrix}^T \otimes \begin{bmatrix} D_G^h(x, Q^2) \\ D_\lambda^h(x, Q^2) \\ D_{q^{(+)}}^h(x, Q^2) \\ D_{\tilde{q}^{(+)}}^h(x, Q^2) \end{bmatrix}. \quad (17)$$

To solve for all the flavours, it is convenient to introduce the linear combinations

$$\begin{aligned} \chi_i(x, Q^2) &= D_{q_i^{(+)}}^h - \frac{1}{n_f} D_{q^{(+)}}^h \\ \tilde{\chi}_i(x, Q^2) &= D_{\tilde{q}_i^{(+)}}^h - \frac{1}{n_f} D_{\tilde{q}^{(+)}}^h \end{aligned} \quad (18)$$

and the additional singlet equations

$$\begin{aligned} Q^2 \frac{d}{dQ^2} D_{q_i^{(-)}}(x, Q^2) &= \frac{\alpha(Q^2)}{2\pi} \left(P_{qq} \otimes D_{q_i^{(-)}}^h + P_{\tilde{q}q} \otimes D_{\tilde{q}_i^{(-)}}^h \right) \\ Q^2 \frac{d}{dQ^2} D_{\tilde{q}_i^{(-)}}(x, Q^2) &= \frac{\alpha(Q^2)}{2\pi} \left(P_{q\tilde{q}} \otimes D_{q_i^{(-)}}^h + P_{\tilde{q}\tilde{q}} \otimes D_{\tilde{q}_i^{(-)}}^h \right) \end{aligned} \quad (19)$$

and

$$\begin{aligned} Q^2 \frac{d}{dQ^2} D_{\chi_i}^h(x, Q^2) &= \frac{\alpha(Q^2)}{2\pi} \left(P_{qq} \otimes D_{\chi_i}^h + P_{\tilde{q}q} \otimes D_{\tilde{\chi}_i}^h \right) \\ Q^2 \frac{d}{dQ^2} D_{\tilde{\chi}_i}^h(x, Q^2) &= \frac{\alpha(Q^2)}{2\pi} \left(P_{q\tilde{q}} \otimes D_{\chi_i}^h + P_{\tilde{q}\tilde{q}} \otimes D_{\tilde{\chi}_i}^h \right). \end{aligned} \quad (20)$$

The general flavour decomposition is obtained by solving the singlet equations for $D_{q^{(+)}}^h$ and $D_{\tilde{q}^{(+)}}^h$, then solving the non-singlet equations for $D_{q_i^{(-)}}^h$ and $D_{\tilde{q}_i^{(+)}}^h$ and for $D_{\chi_i}^h$ and $D_{\tilde{\chi}_i}^h$. At a second step we solve the singlet equations for $D_{q^{(+)}}^h$ and $D_{\tilde{q}}^h$ and use the relations

$$\begin{aligned} D_{q_i}^h &= \frac{1}{2} \left(D_{q_i^{(-)}}^h + D_{\chi_i}^h + \frac{1}{n_f} D_{q^{(+)}}^h \right) \\ D_{\tilde{q}_i}^h &= -\frac{1}{2} \left(D_{q_i^{(-)}}^h - D_{\chi_i}^h - \frac{1}{n_f} D_{q^{(+)}}^h \right) \end{aligned} \quad (21)$$

and

$$\begin{aligned} D_{\tilde{q}_i}^h &= \frac{1}{2} \left(D_{\tilde{q}_i^{(-)}}^h + D_{\tilde{\chi}_i}^h + \frac{1}{n_f} D_{\tilde{q}^{(+)}}^h \right) \\ D_{\tilde{\chi}_i}^h &= -\frac{1}{2} \left(D_{\tilde{q}_i^{(-)}}^h - D_{\tilde{\chi}_i}^h - \frac{1}{n_f} D_{\tilde{q}^{(+)}}^h \right) \end{aligned} \quad (22)$$

to identify the various flavor components.

3 The Spacelike Kernels

$$P_{AP}^S = \begin{bmatrix} P_{gg} & 0 & P_{gq} & 0 \\ 0 & 0 & 0 & 0 \\ P_{qg} & 0 & P_{qq} & 0 \\ 0 & 0 & 0 & 0 \end{bmatrix} \quad (23)$$

$$P_{SAP}^S = \begin{bmatrix} P_{gg} & P_{g\lambda} & P_{gq} & 0 \\ P_{\lambda g} & P_{\lambda\lambda} & P_{\lambda q} & 0 \\ P_{qg} & P_{q\lambda} & P_{qq} & 0 \\ 0 & 0 & 0 & 0 \end{bmatrix} \quad (24)$$

$$P_{ESAP}^S = \begin{bmatrix} P_{gg} & P_{g\lambda} & P_{gq} & P_{gs} \\ P_{\lambda g} & P_{\lambda\lambda} & P_{\lambda q} & P_{\lambda s} \\ P_{qg} & P_{q\lambda} & P_{qq} & P_{qs} \\ P_{sq} & P_{s\lambda} & P_{sq} & P_{ss} \end{bmatrix} \quad (25)$$

Their LO expressions are given by

$$\begin{aligned} P_{qq}^{(0)} &= C_F \left(\frac{1+x^2}{1-x} \right)_+ \\ P_{qq}^{(0)}(x) &= P_{qq,NS}^{(0)} \\ P_{qg}^{(0)}(x) &= 2T_R n_f (x^2 + (1-x)^2) \\ P_{gq}^{(0)}(x) &= C_F \frac{1+(1-x)^2}{x} \\ P_{gg}^{(0)}(x) &= 2N_c \left(\frac{1}{(1-x)_+} + \frac{1}{x} - 2 + x(1-x) \right) + \frac{\beta_0}{2} \delta(1-x) \end{aligned} \quad (26)$$

The SAP kernels are given by

$$P_{gg}^{(0)} = 2C_A \left[\frac{1}{(1-x)_+} + \frac{1}{x} - 2 + x(1-x) \right] + \frac{\beta_0^S}{2} \delta(1-x)$$

$$\begin{aligned}
P_{g\lambda}^{(0)} &= C_\lambda \left[\frac{1 + (1-x)^2}{x} \right] \\
P_{gq}^{(0)} &= P_{gq}^{(0)} = C_F \left[\frac{2}{x} - 2 + x \right] \\
P_{\lambda g}^{(0)} &= n_\lambda [1 - 2x + 2x^2] \\
P_{\lambda\lambda}^{(0)} &= C_\lambda \left[\frac{2}{(1-x)_+} - 1 - x + \frac{3}{2}\delta(1-x) \right] = C_\lambda \left(\frac{1+x^2}{(1-x)_+} \right) \\
P_{\lambda q}^{(0)} &= C_\lambda(1-x) \\
P_{qg}^{(0)} &= P_{qg}^{(0)} = n_f [x^2 + (1-x)^2] \\
P_{q\lambda}^{(0)} &= n_f(1-x) \\
P_{qq}^{(0)} &= C_F \left[\frac{(1+x^2)}{(1-x)_+} \right] \\
&= C_F \left(\frac{2}{(1-x)_+} - 1 - x + \frac{3}{2}\delta(1-x) \right)
\end{aligned} \tag{27}$$

The ESAP kernels are given by

$$\begin{aligned}
P_{\lambda g}^{(0)} &= n_\lambda [2x - 1] \\
P_{\lambda\lambda}^{(0)} &= C_A \left[\frac{2}{(1-x)_+} - 1 - x \right] + \left(\frac{3}{2}C_A - \frac{T_R}{2} \right) \delta(1-x) \\
P_{\lambda q}^{(0)} &= C_\lambda(1-x) \\
P_{\lambda s}^{(0)} &= C_F \\
P_{qg}^{(0)S} &= P_{qg}^{(0)} = n_f [x^2 + (1-x)^2] \\
P_{q\lambda}^{(0)} &= n_f(1-x) \\
P_{qq}^{(0)S} &= C_F \left[\left(\frac{(1+x^2)}{(1-x)_+} \right) - \frac{1}{2}\delta(1-x) \right]_+
\end{aligned}$$

$$\begin{aligned}
&= C_F \left(\frac{2}{(1-x)_+} - 1 - x + \frac{3}{2} \delta(1-x) \right) \\
P_{qs}^{(0)} &= C_F \\
P_{sg}^{(0)} &= n_f [1 - (x^2 + (1-x)^2)] \\
P_{s\lambda}^{(0)} &= n_f x \\
P_{sq}^{(0)} &= C_F x \\
P_{ss}^{(0)} &= C_F \left(\frac{2}{(1-x)_+} - 2 \right) + C_F \delta(1-x)
\end{aligned}
\tag{28}$$

Sum Rules

The moments are defined by

$$P(n) \equiv \int_0^1 dx x^{n-1} P(x) \quad (29)$$

$$\langle q_v(Q^2) \rangle_1 = \langle q_v(Q_0^2) \rangle_1, \quad (30)$$

valid for $Q_0 \leq Q \leq m_{\tilde{q}}$, where $m_{\tilde{q}} \geq m_{2\lambda}$.

For $Q > m_{\tilde{q}}$, the ESAP evolution is given by

$$Q^2 \frac{d}{dQ^2} \begin{bmatrix} \langle q_V \rangle_1 \\ \langle \tilde{q}_V \rangle_1 \end{bmatrix} = \frac{\alpha(Q^2)}{2\pi} \begin{bmatrix} -\frac{1}{2} & 1 \\ \frac{1}{2} & -1 \end{bmatrix} \begin{bmatrix} \langle q_V \rangle_1 \\ \langle s_V \rangle_1 \end{bmatrix} \quad (31)$$

The matrix has a zero eigenvalue corresponding to conservation of baryon number

$$\int_0^1 dx (q_v(x, Q^2) + \tilde{q}_v(x, Q^2)) = 3 \quad (32)$$

and admits a solution of the form

$$\begin{aligned} \langle q_v(Q^2) \rangle_1 &= 2 + \left(\frac{\alpha(Q^2)}{\alpha(Q_0^2)} \right)^{3C_F/\beta_0^{ES}} \\ \langle \tilde{q}_v(Q^2) \rangle_1 &= 1 - \left(\frac{\alpha(Q^2)}{\alpha(Q_0^2)} \right)^{3C_F/\beta_0^{ES}}. \end{aligned} \quad (33)$$

The first stage of the evolution (QCD interval) involves the sum rule

$$\int_0^1 dx (xG(x, Q^2) + xq^{(+)}(x, Q^2)) = 1 \quad (34)$$

valid below the $m_{2\lambda}$.

Moving above the 2-gluino threshold the momentum sum rule becomes

$$\int_0^1 dx (xG(x, Q^2) + x\lambda(x, Q^2) + xq^{(+)}(x, Q^2)) = 1 \quad (35)$$

$$\begin{aligned} \langle q(Q^2) \rangle_2 &= \frac{3n_f}{16 + 3n_f} + \left(\langle q(Q^2) \rangle_2 - \frac{3n_f}{16 + 3n_f} \right) \left(\frac{\alpha(Q^2)}{\alpha(Q_0^2)} \right)^{\frac{2}{\beta_0}(16/9+n_f/3)} \\ \langle q(Q^2) \rangle_2 &= \frac{16}{16 + 3n_f} + \left(\langle q(Q^2) \rangle_2 - \frac{3n_f}{16 + 3n_f} \right) \left(\frac{\alpha(Q^2)}{\alpha(Q_0^2)} \right)^{\frac{2}{\beta_0}(16/9+n_f/3)} \end{aligned} \quad (36)$$

At extremely large Q , in the asymptotic limit, the general partition of momentum due to the partial supersymmetric evolution (SAP) are given by

$$\begin{aligned} \int_0^1 dx xq(x, Q^2) &\rightarrow \frac{3 (16 \langle G(m_{2\lambda}^2) \rangle_2 + 3 n_f \langle q(m_{2\lambda}^2) \rangle_2)}{48 + 9 n_f + 4 n_l} \\ \int_0^1 dx xG(x, Q^2) &\rightarrow \frac{48 (\langle G(m_{2\lambda}^2) \rangle_2 + \langle q(m_{2\lambda}^2) \rangle_2)}{48 + 9 n_f + 4 n_\lambda} \\ \int_0^1 dx x\lambda(x, Q^2) &\rightarrow \frac{4 n_\lambda (\langle q(m_{2\lambda}^2) \rangle_2 + \langle G(m_{2\lambda}^2) \rangle_2)}{48 + 9 n_f + 4 n_\lambda} \end{aligned} \quad (37)$$

If we assume that at the lower boundary all the momentum is carried by the quarks, and neglect the gluonic contribution, then

the equations above have the asymptotic limits

$$\begin{aligned}
\int_0^1 dx xq(x, Q^2) &\rightarrow \frac{9 n_f}{48 + 9 n_f + 4 n_\lambda} \\
\int_0^1 dx xG(x, Q^2) &\rightarrow \frac{48}{48 + 9 n_f + 4 n_\lambda} \\
\int_0^1 dx x\lambda(x, Q^2) &\rightarrow \frac{4 n_\lambda}{48 + 9 n_f + 4 n_\lambda}. \quad (38)
\end{aligned}$$

The asymptotic ($Q \rightarrow \infty$) values of the distribution of momentum are easily derived (we set $\tilde{q}^+(m_{\tilde{q}}) = 0$ at the susy threshold)

$$\begin{aligned}
\int_0^1 dx xG(x, Q^2) &\rightarrow 6 \frac{C_F}{T_R} \frac{2 (G(m_{2\lambda}^2) + \lambda(m_{2\lambda}^2) + q^+(m_{2\lambda}^2))}{5(3 C_F + T_R)} \\
\int_0^1 dx x\lambda(x, Q^2) &\rightarrow 3 \frac{C_F}{2T_R} \frac{2 (G(m_{2\lambda}^2) + \lambda(m_{2\lambda}^2) + q^+(m_{2\lambda}^2))}{5(3 C_F + T_R)} \\
\int_0^1 dx xq^+(x, Q^2) &\rightarrow \frac{3 (G(m_{2\lambda}^2) + \lambda(m_{2\lambda}^2) + q^+(m_{2\lambda}^2))}{5(3 C_F + T_R)} \\
\int_0^1 dx x\tilde{q}(x, Q^2) &\rightarrow \frac{2 (G(m_{2\lambda}^2) + \lambda(m_{2\lambda}^2) + q^+(m_{2\lambda}^2))}{5(3 C_F + T_R)}
\end{aligned} \quad (39)$$

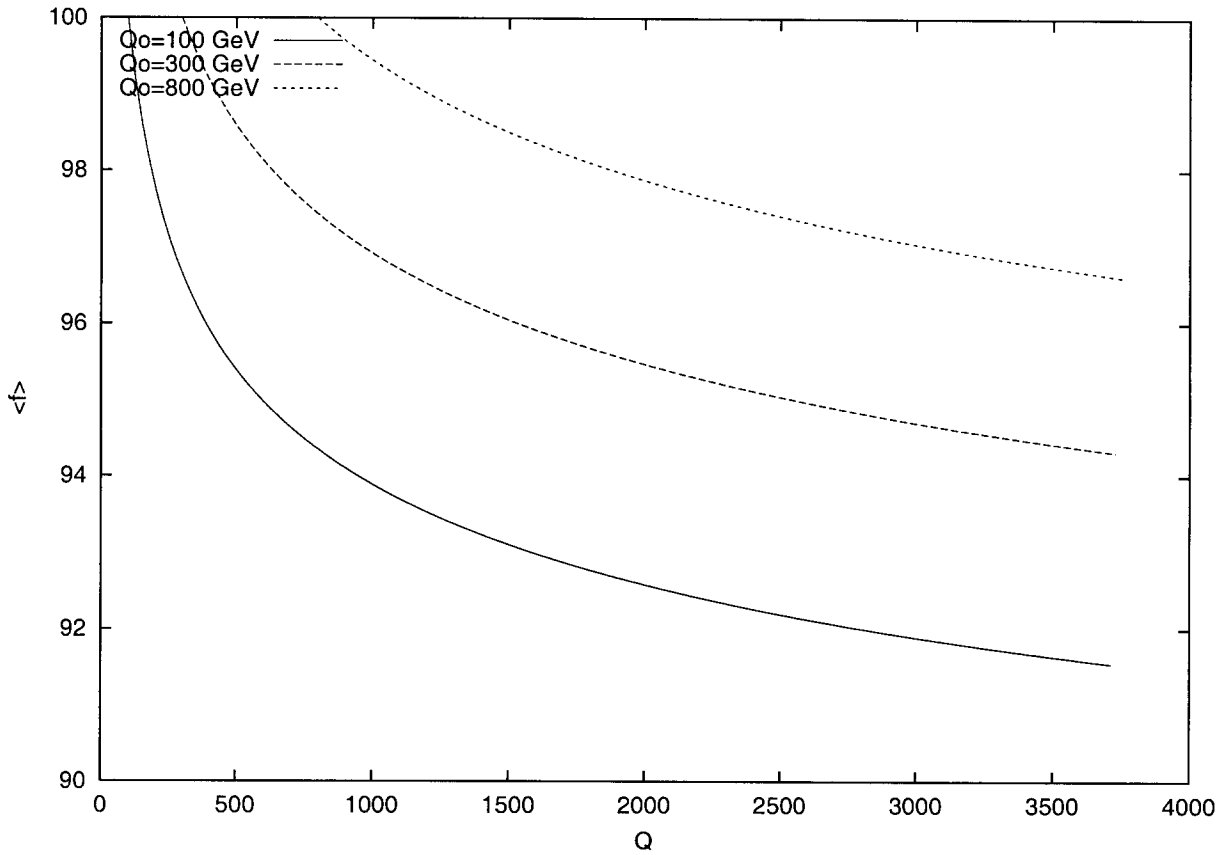


Figure 2: $\langle q(x, Q^2) \rangle_1$ for 3 different matching scales $Q_0 = m_{\bar{q}}$. The 3 scales are chosen to be 100, 300, 800 GeV respectively. The final evolution scale is 3700 GeV

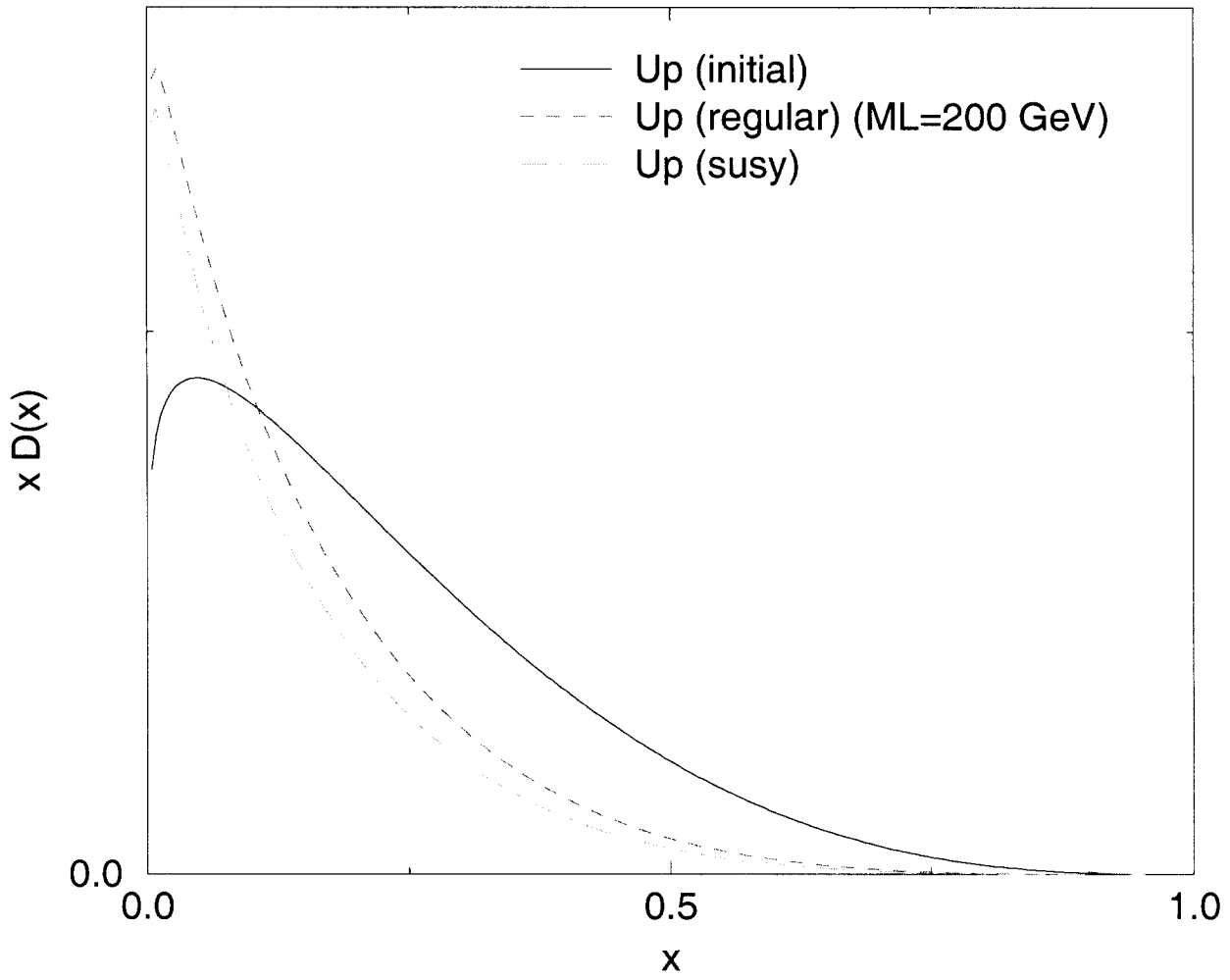


Figure 3: Up quark fragmentation function for $m_\lambda = 200$ GeV, $Q_f = 1000$ TeV

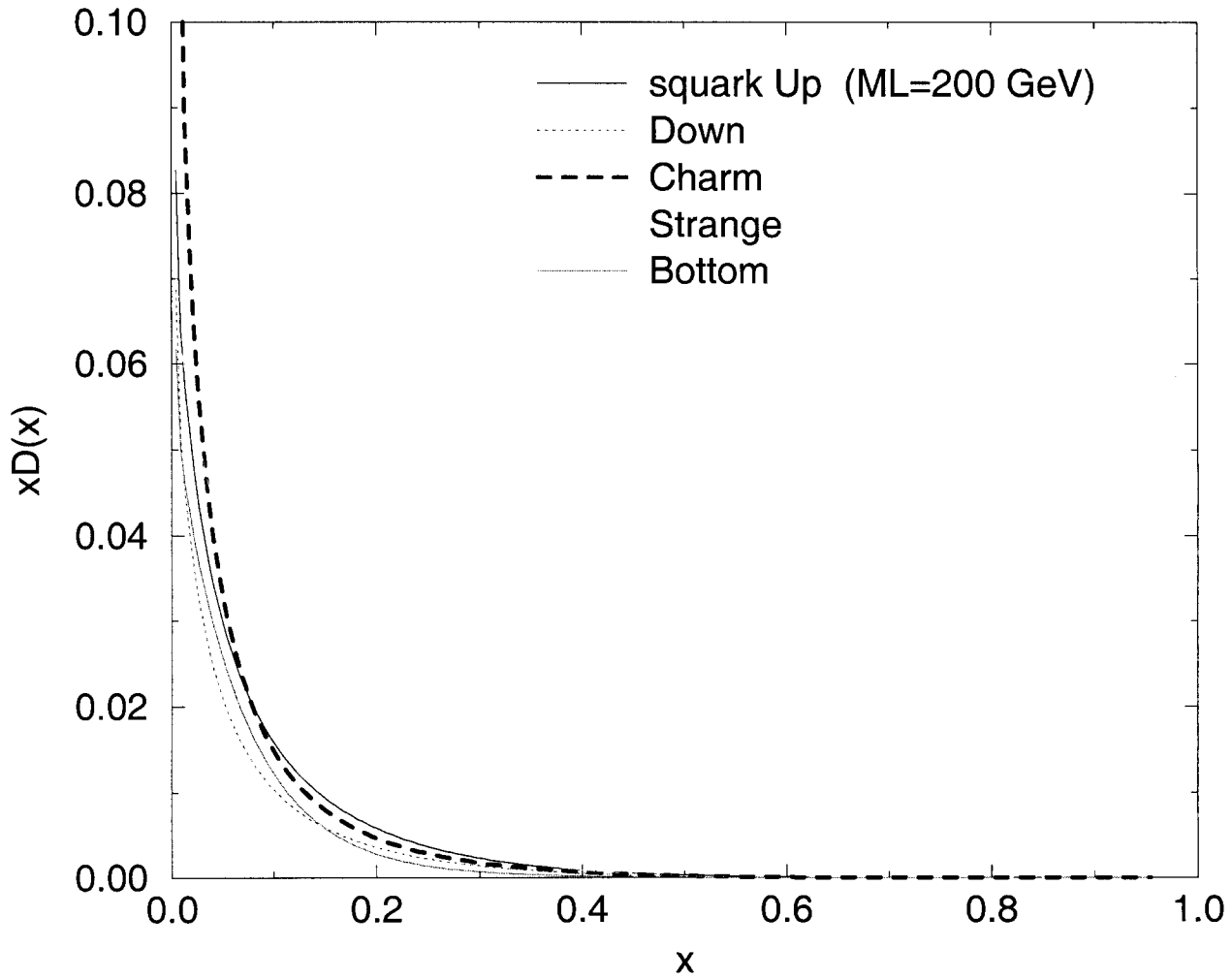


Figure 4: squark fragmentation function for $m_\lambda = 200$ GeV, $Q_f = 1000$ TeV

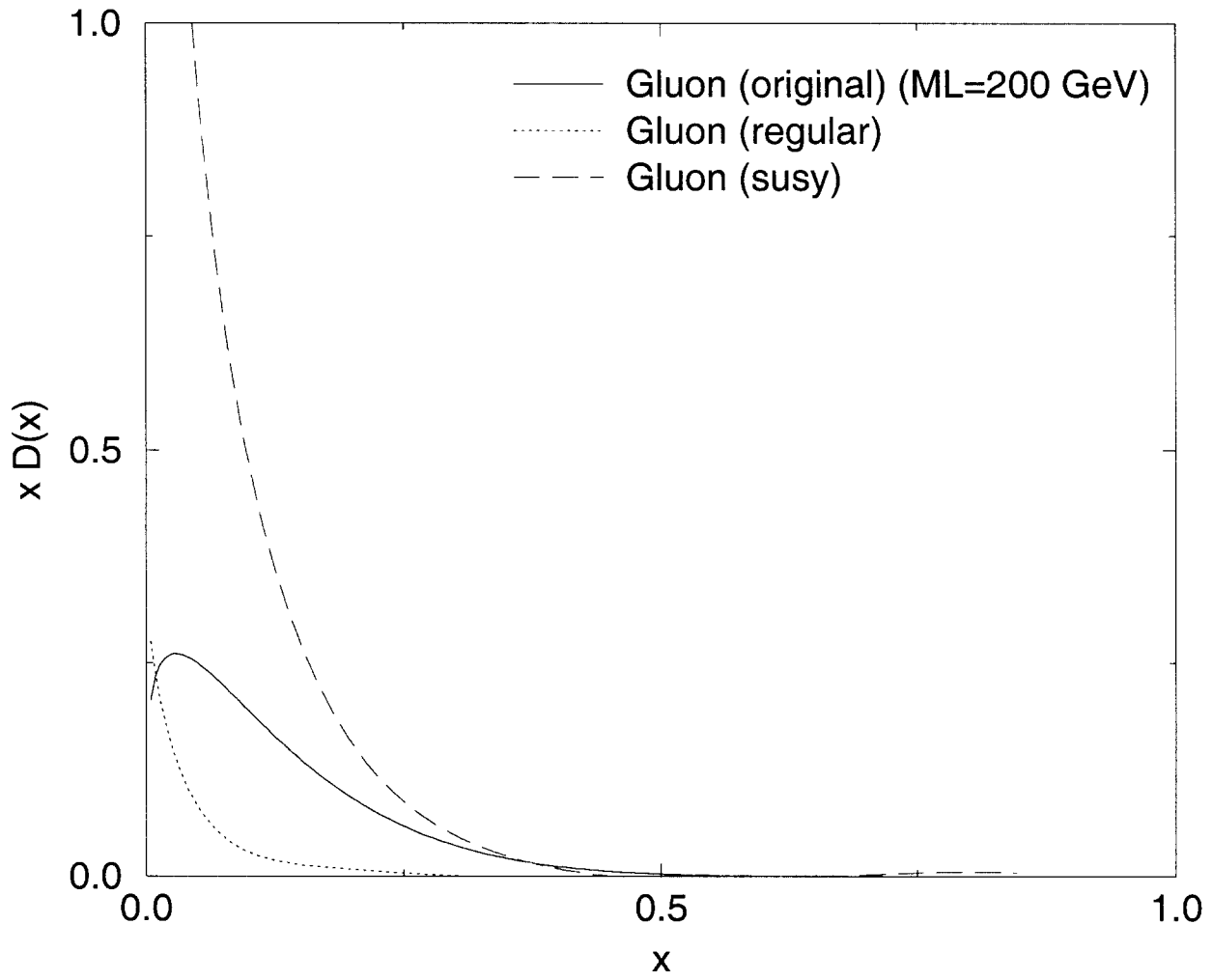


Figure 5: gluon fragmentation function for $m_\lambda = 200$ GeV, $Q_f = 1000$ TeV

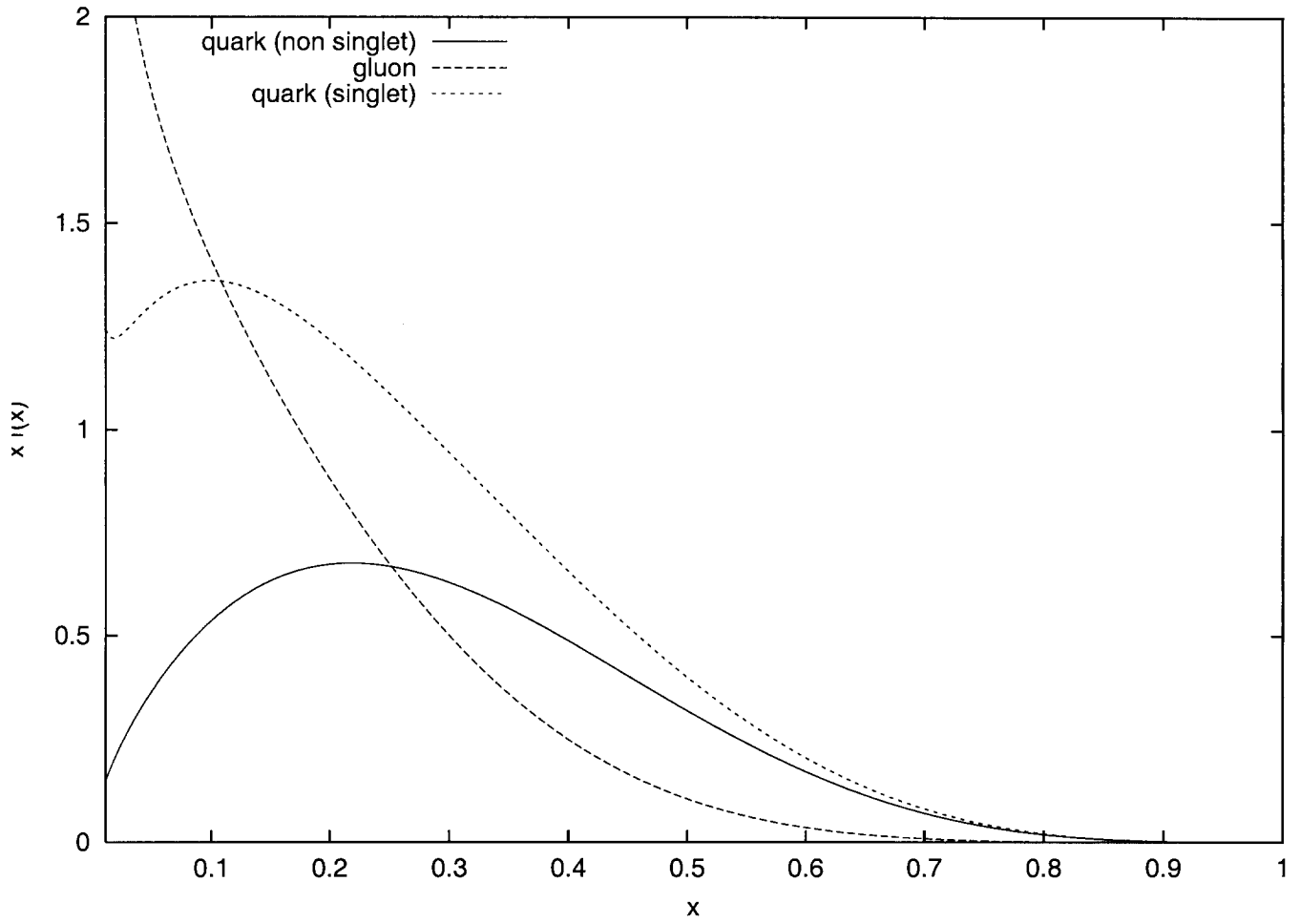


Figure 6: Fig. 1. $xu_v(x)$, $xG(x)$ and $xq^{(+)}(x) \equiv x\Sigma(x)$ at $Q^2 = 4 \text{ GeV}$

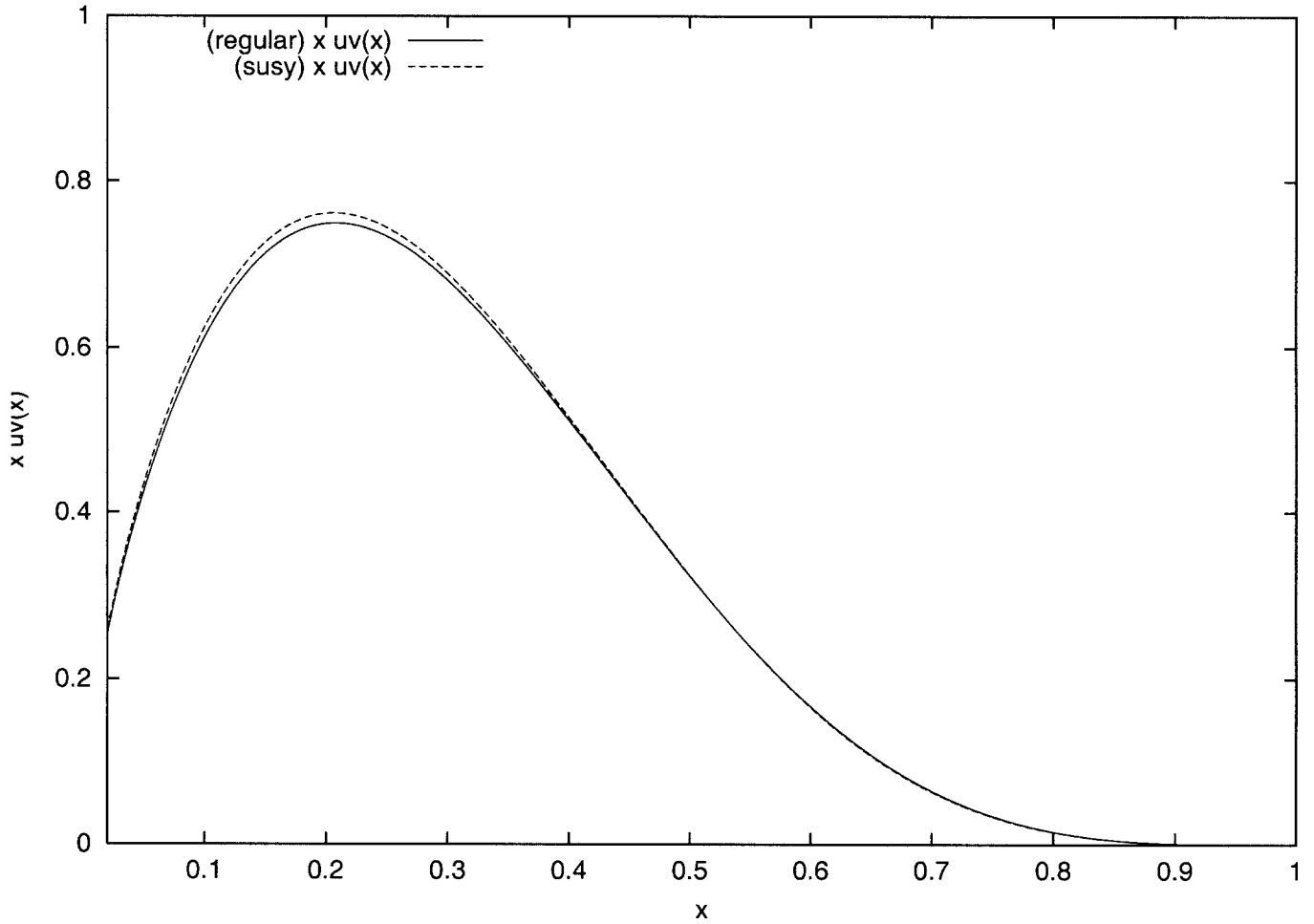


Figure 7: Fig. 2. $xu_v(x)$ evaluated for 4 iterations with $Q_i = 4.0$ GeV and $Q_f = 100$ GeV with $m_\lambda = 2$ GeV in the standard (non-susy) and susy evolution

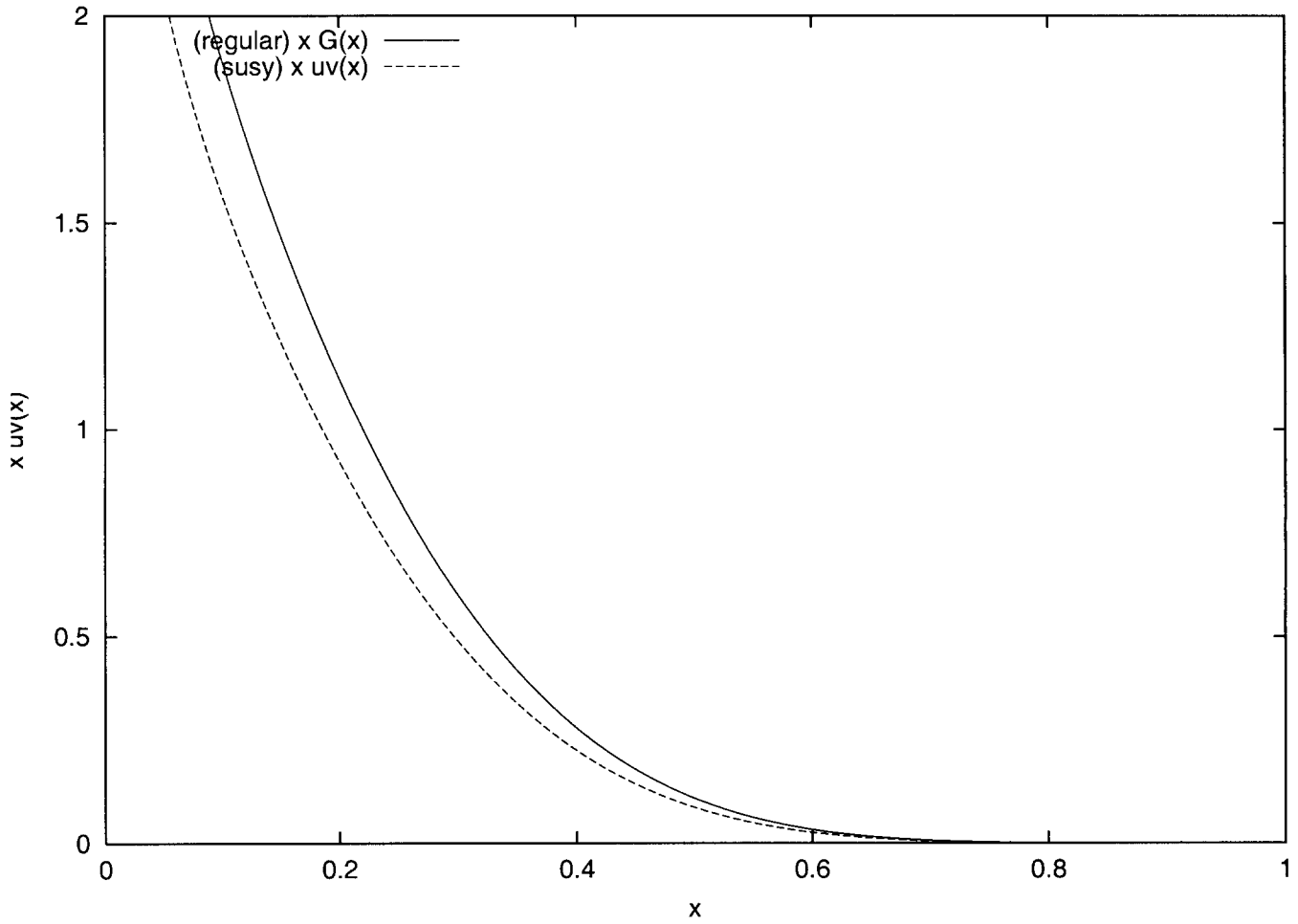


Figure 8: Fig. 3. Gluon distributions with $Q_i^2 = 4.0$ GeV and $Q_f^2 = 100$ GeV with intermediate $m_\lambda = 2$ GeV. The regular and the susy evolution are shown

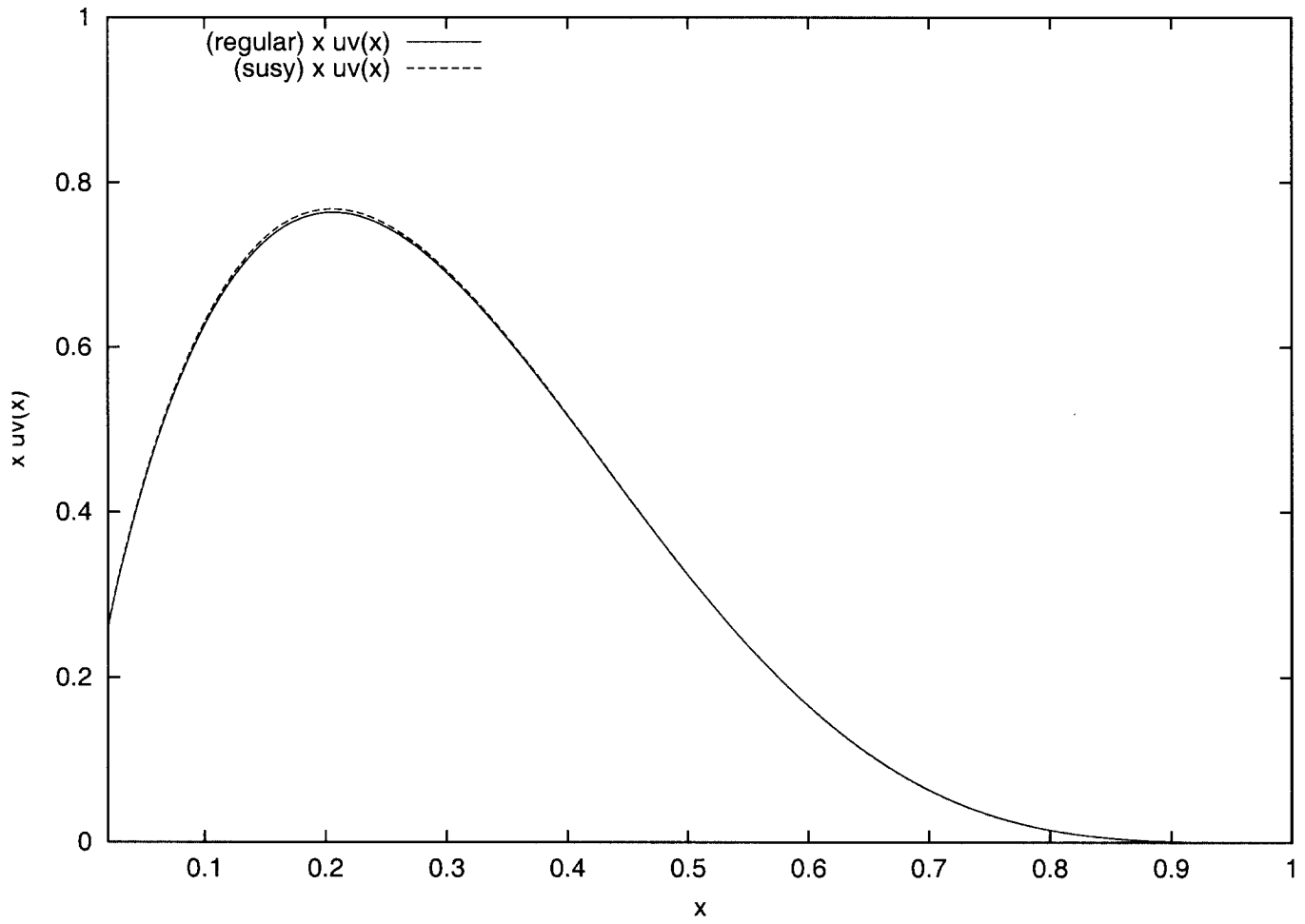


Figure 9: Fig. 4. $xu_v(x)$ evaluated with $Q_i = 4.0$ GeV and $Q_f = 200$ GeV with $m_\lambda = 5$ GeV in the standard (non-susy) and susy evolution

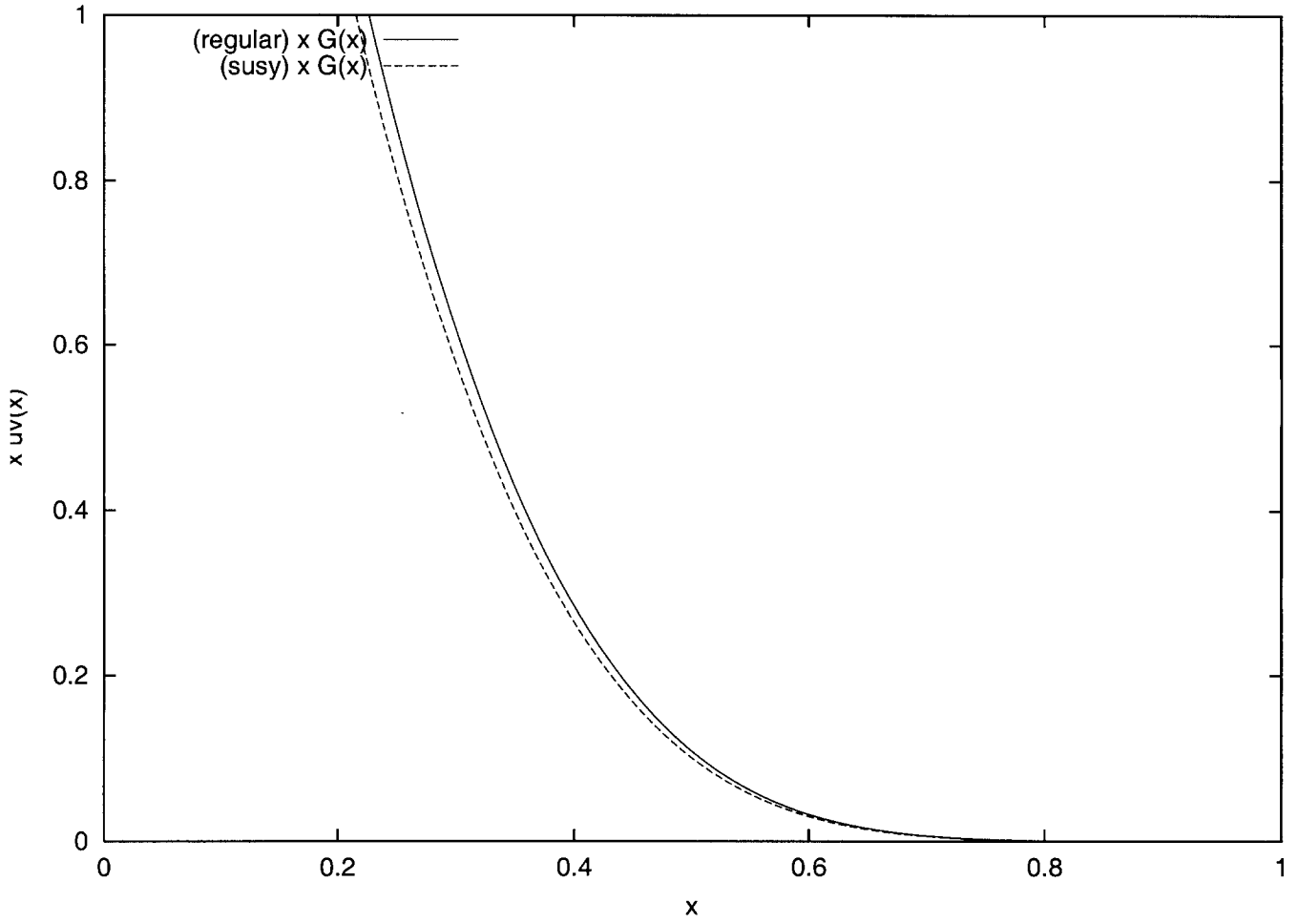


Figure 10: Fig. 5. Gluon distributions with $Q_i^2 = 4.0$ GeV and $Q_f^2 = 200$ GeV with intermediate $m_\lambda = 5$ GeV. The regular and the susy evolution are shown

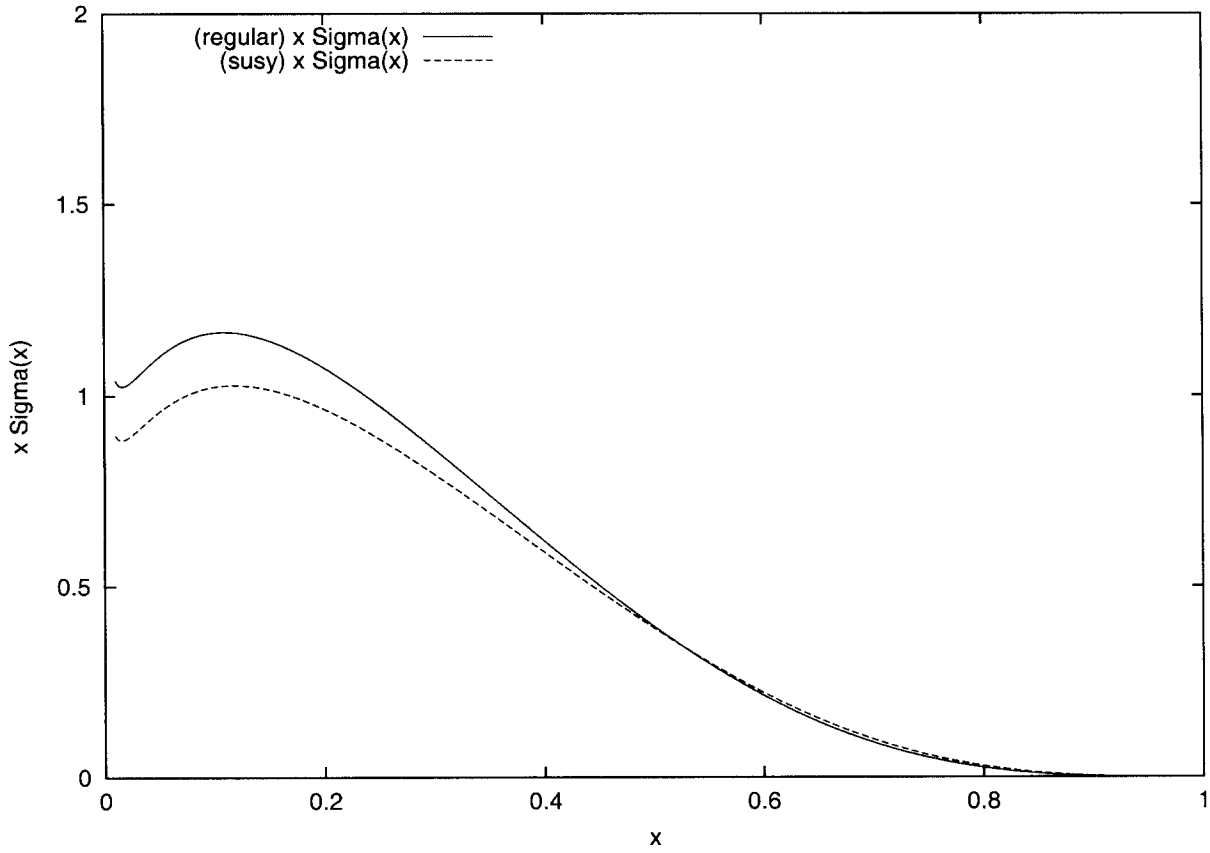


Figure 11: Fig. 6. $x\Sigma(x)$ evaluated with $Q_i^2 = 4.0$ GeV and $Q_f^2 = 200$ GeV with $m_\lambda = 5$ GeV in the standard (non-susy) and susy evolution

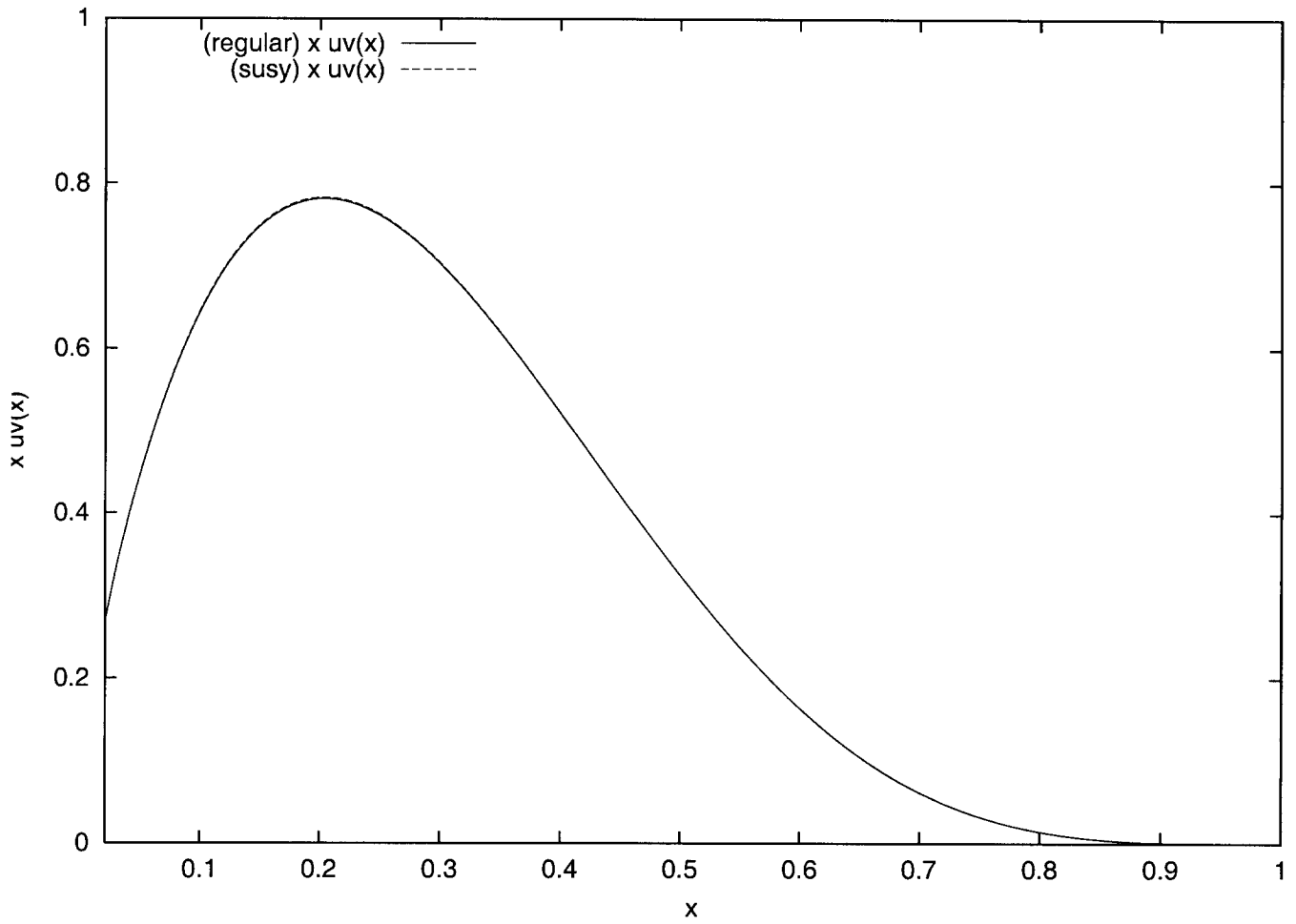


Figure 12: Fig. 7. $xu_v(x)$ evaluated for with $Q_i = 4.0$ GeV and $Q_f = 200$ GeV with $m_\lambda = 10$ GeV in the standard (non-susy) and susy evolution

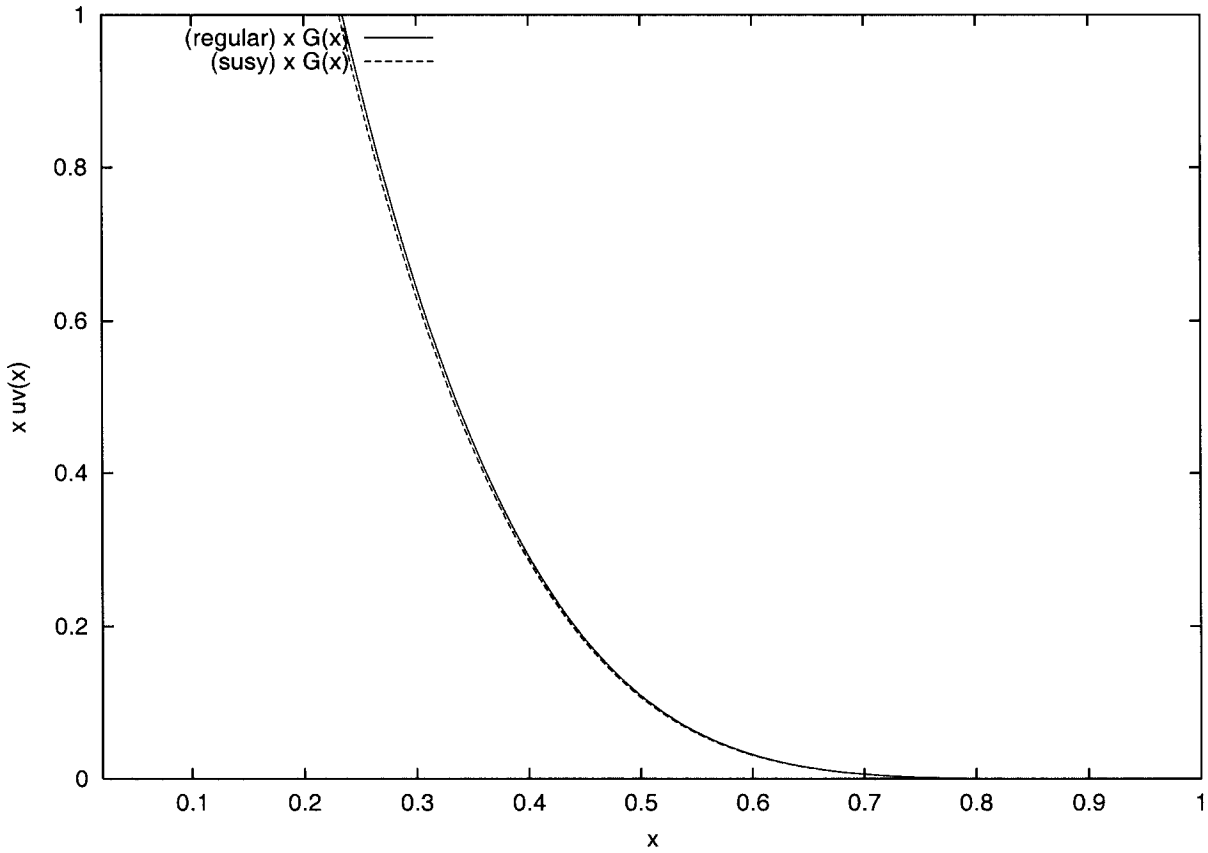


Figure 13: Fig. 8. Gluon distributions with $Q_i^2 = 4.0$ GeV and $Q_f^2 = 200$ GeV with intermediate $m_\lambda = 10$ GeV. The regular and the susy evolution are shown

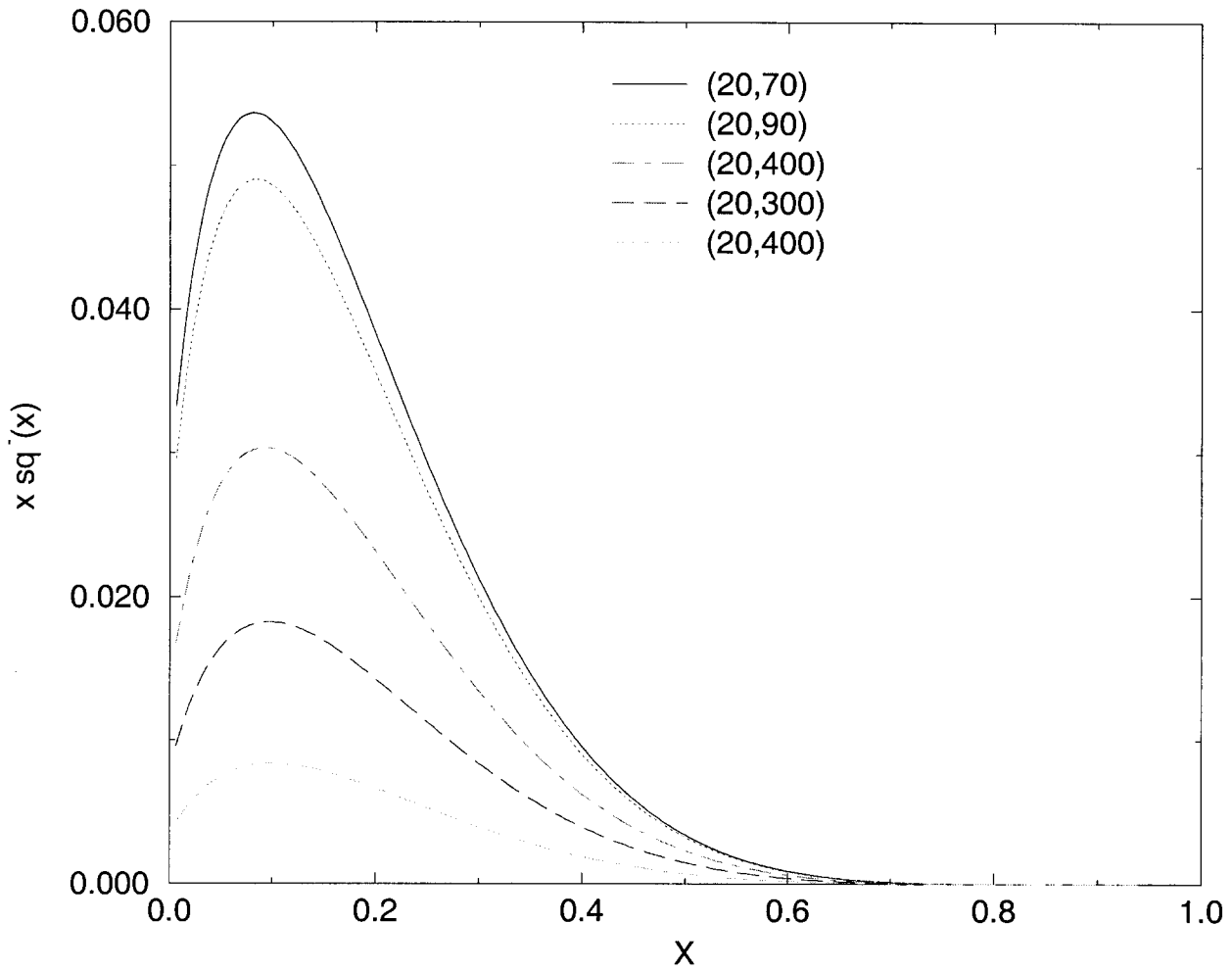


Figure 14: Dependence of the singlet squark distribution on the squark mass for $m_{2\lambda} = 20$ GeV and $m_{\tilde{q}} = 70, 90, 200, 300$ and 400 GeV. We have chosen $Q_f = 500$ TeV

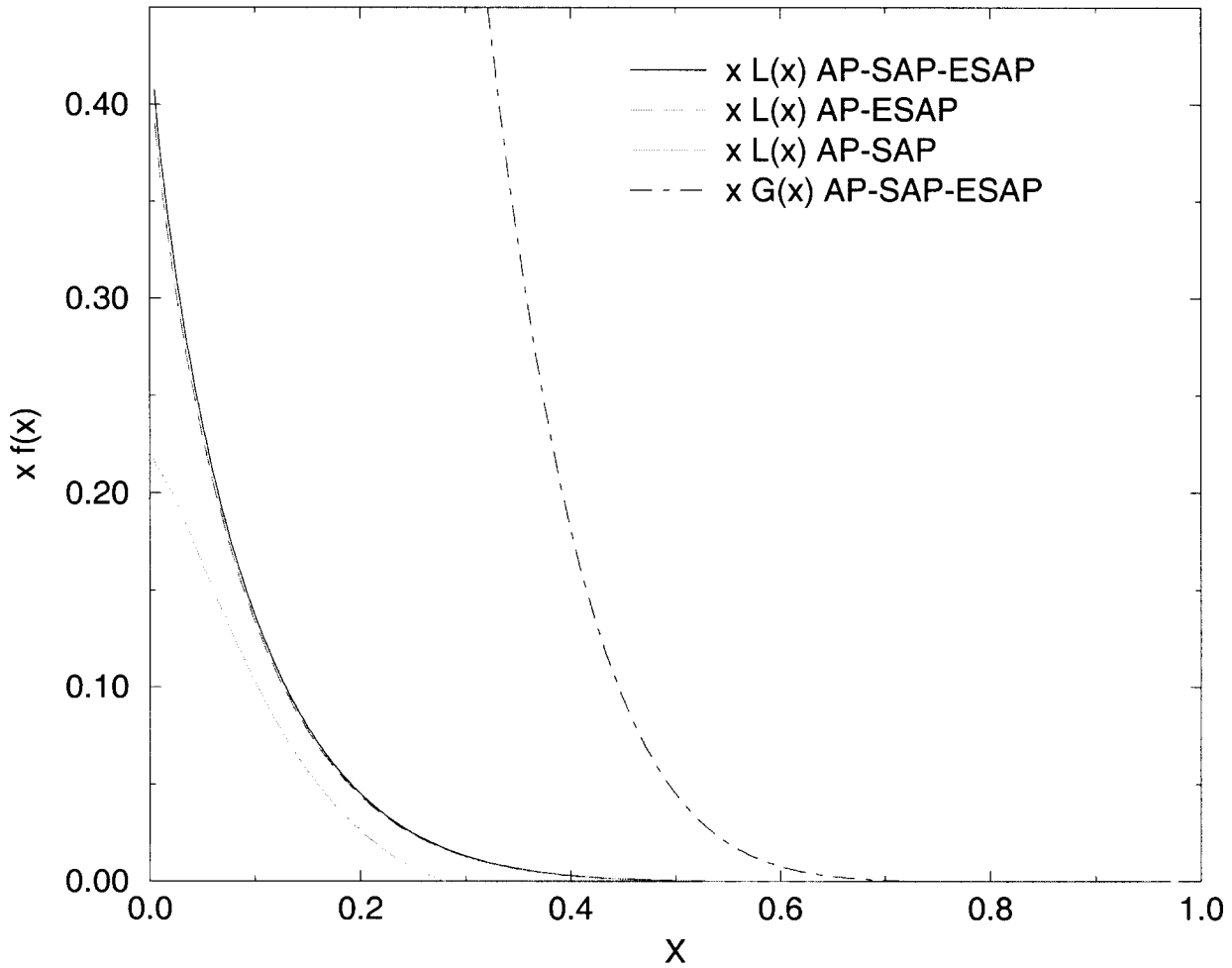


Figure 15: 3 gluino distributions according to the 3 possible evolution models, shown for $m_{2\lambda} = 40$ GeV and $m_{\tilde{q}} = 100$ GeV, and 1 gluon distribution. We have chosen $Q_f = 500$ GeV.

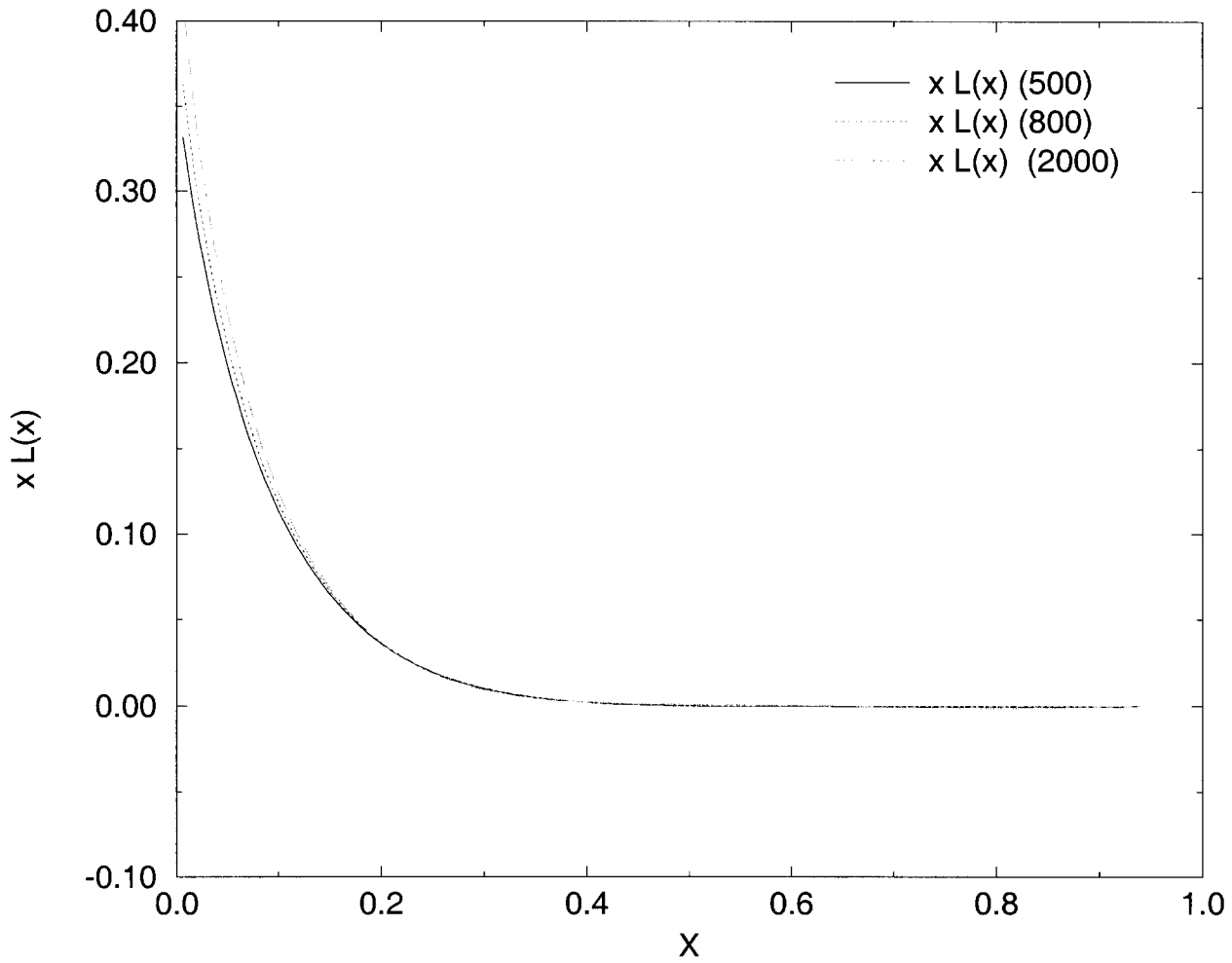


Figure 16: Gluino distribution $x\lambda(x)$ for $m_{2\lambda} = 40$ GeV and $m_{\tilde{q}} = 100$ GeV and $Q_f = 500, 800$ GeV and 2 TeV respectively